Acta Ophthalmologica

Retinitis pigmentosa caused by mutations in the ciliary *MAK* gene is relatively mild and is not associated with apparent extra-ocular features

Ramon A. C. van Huet,[1] Anna M. Siemiatkowska,[2] Riza K. Özgül,[3] Didem Yücel,[3] Carel B. Hoyng,[1] Eyal Banin,[4] Anat Blumenfeld,[4] Ygal Rotenstreich,[5] Frans C. C. Riemslag,[6,7] Anneke I. den Hollander,[1,2,8] Thomas Theelen,[1] Rob W. J. Collin,[2,8] L. Ingeborgh van den Born[6] and B. Jeroen Klevering[1]

[1]Department of Ophthalmology, Radboud University Medical Center, Nijmegen, The Netherlands
[2]Department of Human Genetics, Radboud University Medical Center, Nijmegen, The Netherlands
[3]Institute of Child Health and Metabolism Unit, Department of Pediatrics, Hacettepe University, Ankara, Turkey
[4]Department of Ophthalmology, Hadassah-Hebrew University Medical Center, Jerusalem, Israel
[5]Electrophysiology Clinic, Goldschleger Eye Research Institute, Tel Aviv University, Sheba Medical Centre, Ramat Gan, Israel
[6]The Rotterdam Eye Hospital, Rotterdam, The Netherlands
[7]Bartiméus, Institute for the Visually Handicapped, Zeist, The Netherlands
[8]Nijmegen Center for Molecular Life Sciences, Radboud University Medical Center, Nijmegen, The Netherlands

ABSTRACT.

Purpose: **Defects in *MAK*, encoding a protein localized to the photoreceptor connecting cilium, have recently been associated with autosomal recessive retinitis pigmentosa (RP). The aim of this study is to describe our detailed clinical observations in patients with *MAK*-associated RP, including an assessment of syndromic symptoms frequently observed in ciliopathies.**

Methods: **In this international collaborative study, 11 patients carrying nonsense or missense mutations in *MAK* were clinically evaluated, including extensive assessment of the medical history, slit-lamp biomicroscopy, ophthalmoscopy, kinetic perimetry, electroretinography (ERG), spectral-domain optical coherence tomography (SD-OCT), autofluorescence imaging and fundus photography. Additionally, we used a questionnaire to evaluate the presence of syndromic features and tested the olfactory function.**

Results: ***MAK*-associated RP is not associated with syndromic features, not even with subclinical dysfunction of the olfactory apparatus. All patients experienced typical RP symptoms of night blindness followed by visual field constriction. Symptoms initiated between childhood and the age of 43 (mean: 23 years). Although some patients experienced vision loss, the visual acuity remained normal in most patients. ERG and ophthalmoscopy revealed classic RP characteristics, and SD-OCT demonstrated thinning of the overall retina, outer nuclear layer and photoreceptor–pigment epithelium complex.**

Conclusion: **Nonsense and missense mutations in *MAK* give rise to a non-syndromic recessive RP phenotype without apparent extra-ocular features. When compared to other retinal ciliopathies, *MAK*-associated RP appears to be relatively mild and shows remarkable resemblance to *RP1*-associated RP, which could be explained by the close functional relation of these proteins.**

Key words: clinical variability – MAK – non-syndromic – retinitis pigmentosa

Acta Ophthalmol. 2015: 93: 83–94

doi: 10.1111/aos.12500

Introduction

Retinitis pigmentosa (RP) comprises a group of inherited retinal dystrophies that share clinical characteristics but display an impressive heterogeneity in phenotype and genotype. Symptoms include progressive loss of night vision and peripheral visual field loss that results in tunnel vision. Eventually, patients may lose central vision (Berson 1993; Hartong et al. 2006). Although normal in early stages, the fundus appearance in advanced RP reveals attenuated retinal vessels, waxy pallor of the optic disc, retinal pigment epithelium (RPE) atrophy and bone spicule pigmentations (Berson 1993; Hartong et al. 2006). Full-field electroretinography (ERG) typically shows reduced responses, where rod-driven responses generally are equally or more affected than cone-driven responses.

Mutations in the *MAK* gene, which encodes male germ cell-associated kinase, have recently been associated with retinal degeneration in mice and autosomal recessive RP in humans (Omori et al. 2010; Ozgul et al. 2011; Tucker et al. 2011). The MAK protein is involved in regulating ciliary length in many species (Berman et al. 2003; Bengs et al. 2005; Omori et al. 2010), and non-functional MAK results in

elongation of the photoreceptor connecting cilium, diminished ciliary transport (intraflagellar transport, IFT) and subsequent photoreceptor degeneration in mice (Omori et al. 2010).

Diseases that involve dysfunction of the cilium are generally referred to as ciliopathies (Hildebrandt et al. 2011). They include multi-organ syndromic phenotypes, as the mutated ciliary genes are expressed in multiple tissues (Nigg & Raff 2009; Mockel et al. 2011; Novarino et al. 2011), although mutations in ubiquitously expressed ciliary genes may also result in single organ disease (Estrada-Cuzcano et al. 2012a, b,c). Expression of *MAK* was first identified in murine testicular germ cells (Matsushime et al. 1990). Subsequently, expression in photoreceptors, olfactory receptors and in the epithelium of the respiratory tract and choroid plexus has been shown in mice (Bladt & Birchmeier 1993; Blackshaw et al. 2004). Nevertheless, no syndromic features have been observed in $Mak^{-/-}$ mice (Omori et al. 2010).

In a recent study, Stone et al. described the ophthalmic features observed in 24 *MAK*-associated RP patients. In that study, all but one patient were from Ashkenazi Jewish origin and carried a homozygous 353-base pair insertion in exon 9, which results in loss of the retina-specific isoform of MAK (Stone et al. 2011b). Although the *MAK* exon 9 insertion is the most frequent cause of RP in Ashkenazi Jews, this insertion has so far not been identified in individuals from other origins (Ozgul et al. 2011; Stone et al. 2011b). Detailed clinical features of RP patients carrying missense or nonsense mutations in *MAK* have not been described yet. In addition, the presence of syndromic features has thus far not been evaluated in any *MAK*-related RP patient.

In this report, we describe the clinical results of an international collaborative study that investigated the clinical characteristics and possible syndromic associations of 11 patients with RP caused by nonsense or missense mutations in *MAK*.

Patients and Methods

Patients

Eleven RP patients with mutations in *MAK* from seven families were studied at Hacettepe University in Ankara, Turkey (by RKÖ, family A); the Radboud University Medical Centre in Nijmegen, the Netherlands (by RACvH, CBH and BJK, families B–D); the Rotterdam Eye Hospital in Rotterdam, the Netherlands (by LIvdB and FCCR, family E); the Hadassah-Hebrew University Medical Center in Jerusalem, Israel (by EB, family F) and the Goldschleger Eye Research Institute in Sheba Medical Center, Israel (by YR, family G).

This study adhered to the tenets of the Declaration of Helsinki and informed consent was obtained from all participating patients prior to blood withdrawal and additional ophthalmologic examinations. Prior to this study, we obtained institutional review board approvals.

Genetic analysis

In six families (families A–F), *MAK* mutations were identified as described previously (Ozgul et al. 2011). Genetic analysis using Sanger sequencing of all exons and intron–exon boundaries of *MAK* in the probands of five genetically unsolved families of Iraqi origin resulted in the identification of a homozygous mutation in one family, which was included in this study. The most recent human genome variation society (HGVS) nomenclature was used (http://www.hgvs.org/mutnomen/).

Clinical analysis

Clinical data were collected from the medical records of these patients. Following the identification of causative *MAK* mutations, six patients (families B, C, D and E) were re-evaluated in addition to the data collected during routine visits over the years. Medical history was registered with a focus on age of onset, initial symptoms and overall course of the retinal disorder. Age of onset was defined as the age at which the initial symptom was first noticed by the patient. The initial symptom was defined as the first symptom noted by the patient.

The ophthalmic clinical examination included best-corrected visual acuity (BCVA), slit-lamp biomicroscopy, ophthalmoscopy and fundus photography. Goldmann perimetry was performed using targets V-4e, III-4e, I-4e, I-3e, I-2e and I-1e in all but two patients: patient A-IV:1 underwent a full-field 120 point screening test using the Humphrey Field Analyser II (Carl Zeiss, Dublin, CA, USA); perimetry was unavailable in case F-II:2. Fundus autofluorescence (FAF; Spectralis™, Heidelberg Engineering, Heidelberg, Germany) was performed in six patients with a confocal scanning laser ophthalmoscope. FAF images with a view of 30° and 55° on the central retina were acquired using a confocal scanning laser ophthalmoscope (cSLO) with an optically pumped solid state laser (488 nm) for excitation. All patients underwent a full-field ERG except for patient F-II:2. We performed ERG according the guidelines of the International Society for Clinical Electrophysiology of Vision (ISCEV) (Marmor et al. 2009). Responses were evaluated using local reference values.

Retinal structure

We obtained cross-sectional images along the horizontal meridian of the central retina with commercially available spectral-domain optical coherence tomography (SD-OCT) instruments (Spectralis™, Heidelberg Engineering, Heidelberg, Germany) in eight patients using a 20° single line scan covering the fovea. We quantified thickness of the total retina, the outer nuclear layer (ONL) and photoreceptor–RPE complex (PR+RPE) in 4 *MAK*-related RP patients. For reference purposes, a normal data set for the thickness of all three layers on SD-OCT was obtained from 25 age-matched individuals (mean age: 46 years, range 27–62 years) without retinal or vitreoretinal disease. Thickness measurements of the ONL and the PR+RPE were performed at the foveola and at 0.25, 0.5, 1, 1.5, 2 and 2.5 mm eccentricity from the foveola using the thickness graphs in Heidelberg Eye Explorer software (Heidelberg Engineering, Heidelberg, Germany). The ONL was measured from the outer plexiform layer to the external limiting membrane (ELM); the RP+RPE thickness was measured from the ELM to the Bruch membrane, and the total retinal thickness was measured from vitreous–retinal interface to the Bruch membrane complex (Fig. 1). The reference lines that demarcate the layers were manually set and verified; all thickness measurements were performed by the same operator

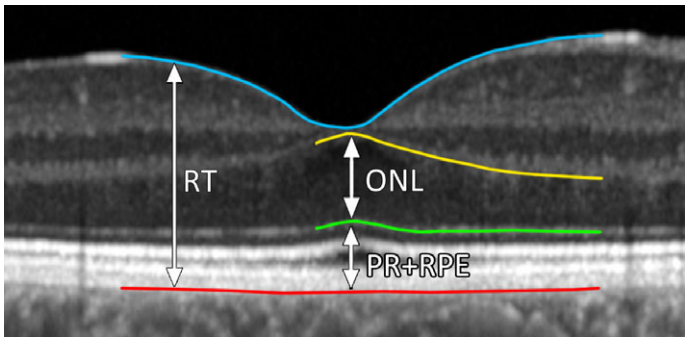

Fig. 1. Illustration of the measured parameters on optical coherence tomography images. The outer nuclear layer (ONL) was measured from the outer border of plexiform layer (yellow line) to the external limiting membrane (ELM, green line). The thickness of the photoreceptor–RPE complex (PR+RPE) was measured from the ELM (green line) to the Bruch membrane (red line), and the total retinal thickness (RT) was measured from the vitreous–retinal interface (blue line) to the Bruch membrane (red line).

(R.A.C.v.H.). Postacquisition interpolation of normal data was performed with custom programs using MatLab (Version R2011a, The MathWorks Incorporated, Natick, MA, USA).

Evaluation of extra-ocular symptoms

To evaluate the presence of syndromic features in the patients with *MAK* mutations, we questioned all patients about the presence of various extra-ocular manifestations covering deficiencies in most tissues that are usually involved in syndromic ciliopathies (Mockel et al. 2011). This questionnaire investigated hearing and balance abnormalities, renal failure or anomalies, cardiac and respiratory anomalies, olfactory deficiencies, polydactyly, obesity, cognitive impairment, fertility disorders, hypogonadism and dental anomalies. Additionally, we assessed olfactory function in six patients using the University of Pennsylvania Smell Identification Test (UPSIT; Sensonics Inc, Haddon Heights, NJ, USA), because olfactory deficiencies frequently go unnoticed by patients (Hoffman et al. 2009) and olfactory functioning might be affected based on the expression of *MAK* in murine olfactory receptors (Bladt & Birchmeier 1993). UPSIT scores were evaluated using the age-matched gender-stratified scoring keys provided in the manual (Doty 1995).

We avoided further invasive procedures to assess the testicular function, as spermatogenesis was normal in *MAK* knockout mice, and sperm motility and male-derived litter sizes were only mildly reduced (Shinkai et al. 2002).

Results

Clinical characteristics

This study included a total of 11 patients (mean age: 50 years) from seven families (Fig. 2). Longitudinal data were available for seven patients (mean duration: 9.3 years). The mean age at onset was 30 years and ranged from childhood to the age of 54, but could not be reliably determined in three patients. The age at diagnosis (mean age: 38 years, range: 20–57 years, $n = 10$) was generally within the first decade after the onset of the disease. All patients noticed night blindness as initial symptom of their disease. In one patient (E-II:1), the molecular diagnosis preceded the visual symptoms after segregation analysis in her family. One year later, she noticed a slightly prolonged adaptation to darkness and minor constriction of her temporal visual field.

An overview of the clinical findings in these patients at the most recent examination is provided in Table 1. The course of the BCVA in the cases with follow-up data is shown in Fig. 3.

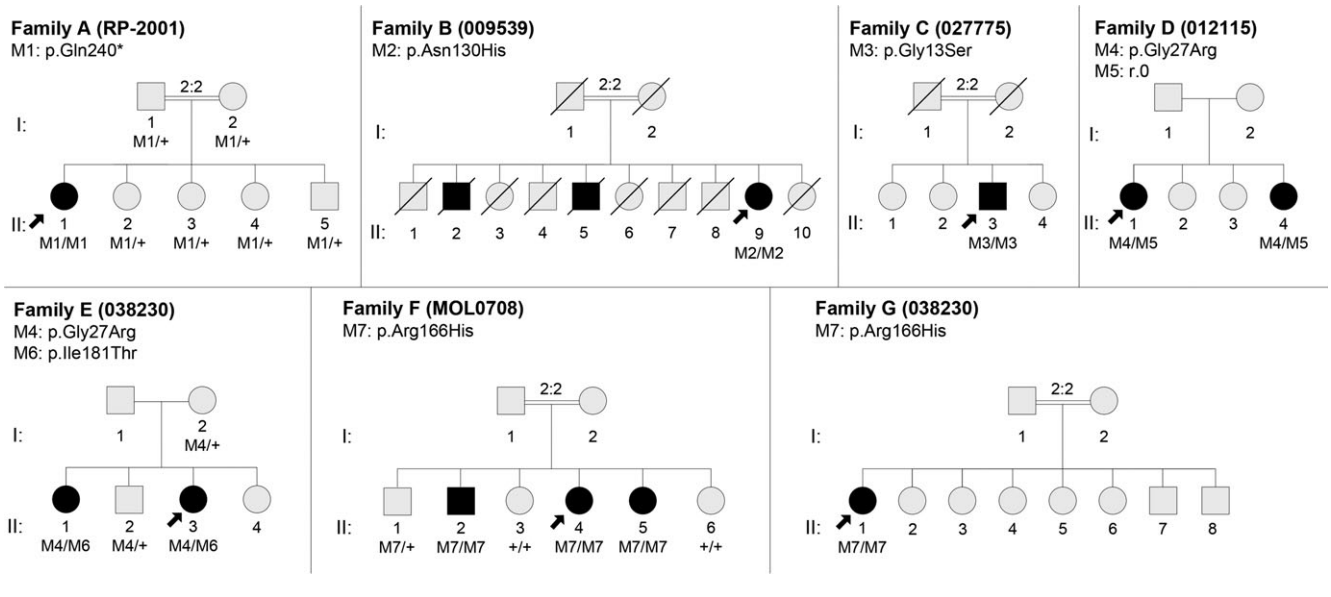

Fig. 2. Revised pedigrees of six families included in this study. Where relatives were available (families A, D and E), the mutation segregates with the disease. Plus signs denote the wild-type allele, square boxes indicate men, circles indicate women, and affected individuals are pointed out in black. An arrow indicates the proband. Double lines point out consanguineous marriages; the numbers above the double lines indicate the degree of consanguinity.

Table 1. Clinical features at most recent examination in patients carrying mutations in *MAK*.

ID/Age of onset (y)/Age/ Sex	Initial symptom	Visual acuity		Lens status	Ophthalmoscopy results	ERG results		Goldmann perimetry	OCT results	Autofluorescence results	Non-ocular findings	Dx	Follow-up (y)
		RE	LE			Scot.	Phot.						
A-IV:1/~20/ 33/F	Night blindness	20/25	20/25	Clear	Scattered pigment accumulations	SR	SR	Constricted VF, central residue: 25°	Irregular foveal photoreceptor reflectance. Otherwise normal.	Hypoautofluorescent lesions in midperiphery,	None	RP	0
B-II:9/~57/ 74/F	Night blindness	HM	HM	Pseudophakia	Large parafoveal lesions of RPE atrophy, RPE changes in remaining posterior pole, attenuated vessels, waxy pallor of the optic disc, bone spicules in midperiphery, RPE atrophy anterior of vascular arcades	NR	NR	Constricted VF, central residue: 20°, severe central sensitivity loss	Severely loss of photoreceptor–RPE complex. Central photoreceptor residue. Diffuse thinning of central retina.	Large hypoautofluorescent lesions and diffuse hyperautofluorescence in posterior pole. Multiple hypoautofluorescent lesions in midperiphery	None	RP	17
C-II:3/17/ 41/M	Night blindness	20/ 125	20/200	Polar posterior cataract	Severely attenuated vessels, waxy pallor of the optic disc, sporadic bone spicules in superotemporal and superonasal midperiphery, RPE atrophy anterior of the vascular arcades, wrinkling of ILM just nasal of fovea	NR	NR	Constricted VF, central residue: 20°, moderate central sensitivity loss	Loss of photoreceptor reflectance peripheral of fovea. ERM with retinal wrinkling.	Parafoveal hyperautofluorescent ring. Hypoautofluorescent lesions in posterior pole, midperiphery and peripapillary region.	None	RP	18.5
D-II:1/45/ 72/F	Night blindness	20/25	20/25	Pseudophakia	RPE alterations in the macula, attenuated arterioles, pallor of the optic disc, bone spicules in midperiphery (less densely packed in temporal quadrant compared with the other quadrants), RPE atrophy anterior of vascular arcade	NR	NR	Constricted VF, central residue: 20°, mild central sensitivity loss in LE	Loss of photoreceptor reflectance peripheral of fovea. Atrophy of choriocapillaris, especially in peripapillary region. IS+OS: 65 μm (RE), 71 μm (LE)	Diffuse hypoautofluorescent lesions and blockage of signal by bone spicules in midperiphery.	None	RP	16
D-II:4/43/ 63/F	Night blindness	20/15	20/20	Clear	Normal macula, attenuated arterioles, waxy pallor of the optic disc, bone spicules in nasal midperiphery, RPE atrophy anterior of the vascular arcades	NR	NR	Mild relative constriction of VF, no absolute constriction, normal central sensitivity	Loss of photoreceptor reflectance peripheral of macula. IS+OS: 82 μm (RE), 79 μm (LE)	Hyperautofluorescent ring within vascular arcades. Diffuse small hypoautofluorescent spots in nasal midperiphery. Hypoautofluorescent peripapillary lesion.	None	RP	1
E-II:1/53/ 55/F	Night blindness	20/15	20/22	Clear	Normal macula, mildly attenuated vessels, normal optic disc, mild RPE alterations and sporadic bone spicules in midperiphery. A small region of lattice degeneration in far periphery and laser scars in far periphery.	WNL	WNL	Mild relative constricted VF, normal central sensitivity	Normal	Normal	None	RP	2
E-II:3/ childhood/ 49/F	Night blindness	20/ 200	20/22	RE: Mild PSC LE: Clear	Normal macula (apart from wrinkling of ILM in the RE), attenuated vessels, normal optic disc, bone spicule pigmentations in nasal and inferior midperiphery, RPE atrophy anterior of vascular arcade.	SR (age 43)	WNL (age 43)	Constricted VF, central residue: 10°, sensitivity, mild sensitivity loss in LE	Loss of photoreceptor reflectance peripheral of macula. Diffuse atrophy of choriocapillaris.	Only LE: Hyperautofluorescent ring within vascular arcades. Diffuse hypoautofluorescent spots in midperiphery.	None	RP	6.5

Table 1. (Continued)

ID/Age of onset (y)/Age/ Sex	Initial symptom	Visual acuity		Lens status	Ophthalmoscopy results	ERG results		Goldmann perimetry	OCT results	Autofluorescence results	Non-ocular findings	Dx	Follow-up (y)
		RE	LE			Scot.	Phot.						
F-II:2/NA/ 33/M	Night blindness	20/63	20/50	NA	NA	NA	NA	NA	NA	NA	None	RP	0
F-II:4/NA/ 57/F	Night blindness	20/50	20/32	Aphakic after congenital cataract	Mild pigmentary changes around arcades	SR	SR	Midperipheral scotomas, temporal VF more affect than nasal VF	NA	NA	None	RP	0
F-II:5/NA/ 49/F	Night blindness	20/32	20/25	NA	Posterior pole normal, mild changes in nasal retina	SR	MR	Midperipheral temporal scotoma	NA	NA	None	Sectorial RP	0
G-II:1/6/32/ F	Night blindness	20/25	20/25	Clear	Normal posterior pole, mild attenuation of the vessels, mild waxy pallor of the optic disc, RPE atrophy and bone spicules in the periphery.	SR (age 28)	SR (age 28)	Constricted VF, central residue: 20°, mild central sensitivity loss	Loss of photoreceptor reflectance peripheral of macula. Diffuse atrophy of choriocapillaris.	NA	None	RP	4

All features are present symmetrically, unless mentioned otherwise. Dx = final diagnosis; ERG = electroretinography; ERM = epiretinal membrane; HM = Hand movements; ILM = internal limiting membrane; LE = left eye; MR = moderately reduced; NA = not available; NR = non-recordable; Ph = photopic responses; PSC = posterior subcapsular cataract; RE = right eye; RPE = retinal pigment epithelium; Sc = scotopic responses; SR = severely reduced; VF = visual field; WNL = within normal limits.

The mean BCVA was approximately 20/40 at a mean age of 50. BCVA was ≥20/50 in at least one eye of nine patients and ≥20/25 in six of these cases, including individuals in their seventh or eighth decade of life. We observed a vision impairing stromal haze, which was already reported at the age of 57, in the cornea of the right eye of patient B-II:9. The origin of this haze was not clear. Lens opacities were observed in patient C-II:3 (polar posterior cataract) and patient E-II:3 (mild posterior subcapsular cataract), whereas patients B-II:9, D-II:1 and F-II:4 underwent cataract extraction, the latter patient due to congenital cataract.

Ophthalmoscopy revealed typical RP features including vessel attenuation, waxy pallor of the optic disc and bone spicules in all patients (Fig. 4A–E). In early stages, the nasal and inferior quadrants were predominantly affected, whereas in later stages, the retina in the superior quadrant became affected in a likewise fashion. The temporal retina showed less densely packed bone spicules in end-stage disease (Fig. 4A–B,D–E). The macular region was unaffected in all patients except for patient B-II:9, who, at the age of 74, showed large atrophic chorioretinal lesions (Fig. 4F) with a corresponding low visual acuity of hand movements in both eyes. An earlier examination, at the age of 57, revealed a bull's eye maculopathy.

Autofluorescence imaging (mean age: 51, range: 41–63 years) revealed typical RP features (Fig. 4G–H), including the hyperautofluorescent ring associated with the transitional zone where photoreceptor inner and outer segments are lost (Popovic et al. 2005; Greenstein et al. 2012)(Fig. 4I–J), and hypoautofluorescent lesions in the mid-periphery. Electrophysiological rod- and cone-driven responses were either severely reduced or non-recordable (Fig. 5). In patients E-II:3 and F-II:5, the responses showed a rod–cone pattern, where rod-driven responses were more severely affected than cone-driven responses. ERG responses within the normal limits were obtained in patient E-II:1, although scotopic minimal responses were at the lower end of the normal spectrum.

Perimetric testing revealed that tunnel vision was a prominent feature in six patients (55%): constricted visual fields up to 10° were observed

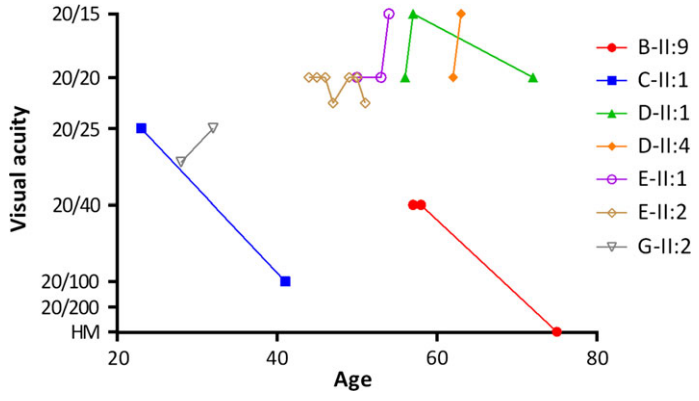

Fig. 3. Best-corrected visual acuity (*y*-axis) related to age (*x*-axis) in seven patients with *MAK*-related retinitis pigmentosa. If visual acuity differed between both eyes, the best visual acuity was used. Small variability in visual acuity was observed in the patients of families D and E. HM, hand movements.

(Table 1). Visual field loss followed the patterns reported earlier (Stone et al. 2011a,b), where no or minor temporal field defects are present in early stages of the disease, whereas in more advanced stages, the field is constricted to a central residue. However, the course of visual field loss was highly variable: patients C-II:3, G-II:1 and E-II:3 had an isolated central residual field (pattern 5) at age 25, 28 and 49, respectively, whereas E-II:1, D-II:1 and D-II:4 had a nearly complete visual field (pattern 1) at age 54, 55 and 63, respectively. Details of visual fields are depicted in Fig. 6. Central sensitivity remained relatively spared in seven patients, which is in accordance with the observed visual acuity (Table 1).

Retinal structure

We observed profound loss of photoreceptor layer structure in the perimacular zone in six patients (mean age: 57; range: 28–74 years). In accordance with the findings at ophthalmoscopy and perimetry, photoreceptor loss was more advanced towards the fovea in the nasal retina compared with the temporal retina (Fig. 4J). In later stages, loss of the photoreceptor layer temporal to the fovea occurred (Fig. 4K).

Thickness measurements are plotted in Fig. 7; normal data were plotted (mean ± 2 SD) as reference for the data from the patients. The overall retina became thinned beyond the fovea in three RP patients, of which two patients also showed a thinned foveal retina. The OCT scan in patient D-II:4 was acquired slightly superior to the foveal dip, resulting in the thickened foveal retina depicted in Fig. 7 (top panel). The other values in this patient were within the normal range due to the early stage of disease. Both ONL and PR+RPE layers were thinned beyond the fovea, except for patient C-II:3 in whom the foveal ONL and PR+RPE thinned as well. Thinning of the retinal, ONL and PR+RPE thickness in the fovea correlated with a decrease in visual acuity. We did not observe thickening of the ONL or PR+RPE layer.

Evaluation of extra-ocular features

All patients were in good general health. No extra-ocular manifestations were reported in the questionnaire and, more specifically, no history of subfertility or infertility was reported in both males included in this study. In the six patients tested with the UPSIT, the absolute ability to smell varied from complete loss (anosmia, patient B-II:9) to normal olfactory function (normosmia, patient D-II:4). However, the absolute ability to smell decreases with age in normal individuals while variance of olfactory function widens, and anosmia is observed in a portion of the normal elderly above the age of 60 (Doty 1995). Compared with age-matched controls, the olfactory function of the six patients tested in this study were all within the normal limits, although often at the lower end (Table 2). None of the patients complained about loss of their ability to smell or taste.

Discussion

MAK has recently been added to the expanding list of genes associated with autosomal recessive RP (Ozgul et al. 2011; Tucker et al. 2011). Pathologic mutations in *MAK* cause abnormal elongation of the cilium, which eventually results in photoreceptor cell death (Omori et al. 2010). Defects in genes involved in ciliary structure or transport are known to cause syndromes that include retinal dystrophy (Campo & Aaberg 1982; Eudy et al. 1998; Zito et al. 2003; Mockel et al. 2011). The exclusion of syndromic abnormalities in *MAK*-associated RP is therefore important. Previously, Stone and co-workers described the retinal phenotype in a genetically homogeneous group of almost exclusively Ashkenazi Jewish patients (Stone et al. 2011a,b). The RP patients in this study carry causative mutations different from the specific insertion described in *MAK* and were not of Ashkenazi Jewish ancestry.

The MAK-associated retinal phenotype

The retinal phenotype of the patients in this study is typical for RP and starts with night blindness and subsequent progressive constriction of the visual field. Visual acuity can remain relatively normal up to late age due to prolonged survival of the central retina, as was observed by Stone et al. (2011a,b). However, in cases B-II:9, C-II:3 and F-II:2, visual acuity decreased to 20/50 or less in both eyes at the age of, respectively, 74, 41 and 57 years, although in case of C-II:3 this may also be explained by visually disturbing cataracts.

In *MAK*-associated RP, visual field loss was initially restricted to the temporal field that gradually progressed to loss of the entire (mid)peripheral field and ends with a isolated central residue. These perimetric findings correlate with the patterns described earlier in *MAK*-related RP by Stone et al. (2011a,b), although we observed only three of five patterns and end-stage pattern 5 was reached at an earlier age by patients C-II:3 and G-II:1 (Fig. 6).

SD-OCT imaging clearly demonstrated the overall thinning of the retina, as well as thinning of the ONL and PR+RPE, whereas foveal thickness initially is spared. PR+RPE thickening

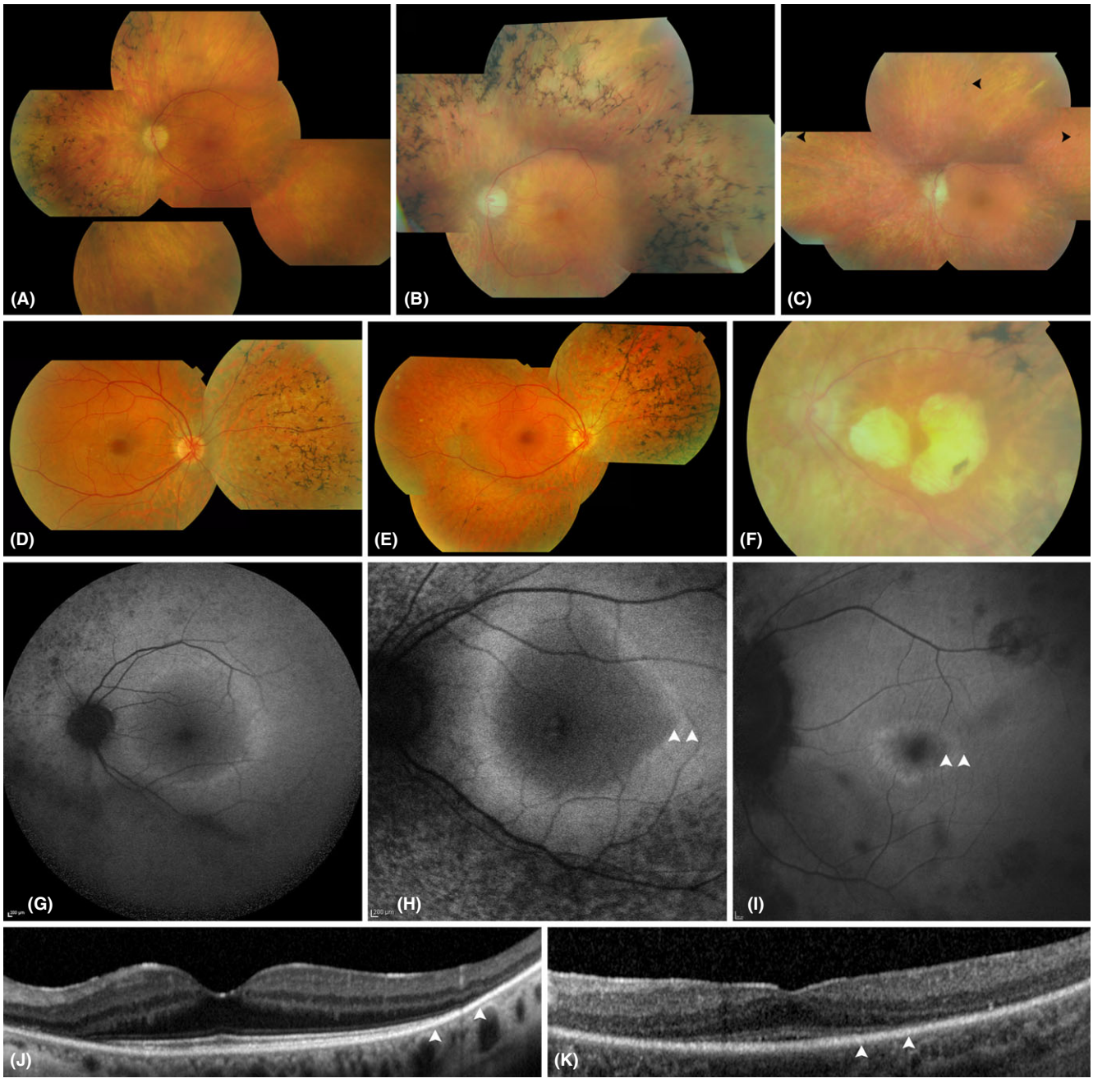

Fig. 4. Fundus photographs and autofluorescence imaging in patients with *MAK*-related retinitis pigmentosa. A, Composition fundus photograph of the left eye of case D-II:4 (age 63) illustrating attenuated vessels, waxy pallor of the optic disc and bone spicule pigmentations in the nasal-superior midperiphery. B, Composition photograph of the left fundus in patient D-:II:1 (age 72) showing attenuated vessels, pallor of the optic disc and bone spicules in the midperiphery. C, Composition fundus photograph of the left eye in patient C-II:3 (age 41) revealing severely attenuated vessels, a pale optic disc amd sporadic bone spicules in superotemporal and superonasal midperiphery (black arrows heads). D/E, Composition fundus photos of the right eye in patient E-II:3 at age 44 (D) and age 46 (E) highlighting the increase in bone spicule pigmentations in the nasal and inferior quadrants as well as the progression in atrophy of the RPE. F, Photograph of the left fundus in patient B-II:9 (age 74) showing large RPE lesions surrounding the fovea, as well as attenuated vessels, waxy pallor of the optic disc and bones spicule pigmentations. G/H, FAF images of the left fundi in patients D-II:4 at age 63 (G) and E-II:3 at age 46 (H) revealing a hyperautofluorescent ring surrounding the normal appearing macula and fine hypoautofluorescent spots in the nasal and superior midperiphery. I, FAF image of the left fundus of case C-II:3 (age 43) revealing a hyperautofluorescent ring around the fovea and irregular hypoautofluorescent spots scattered throughout the posterior pole. J/K, OCT scans along the horizontal meridian of the central retina in patients D-II:4 at age 63 (J) and E-II:3 at age 46 (K) highlighting the remaining photoreceptors and the transitional zone (marked by white arrow heads).

that could accompany the elongation of the connecting cilium to twice its normal length, which was present in rod photoreceptors of *MAK* knockout mice (Omori et al. 2010), was not observed in our patients. This absence of retinal thickening may signify the absence of these structural abnormalities in human photoreceptors, although it cannot be excluded that such thickening lies beyond the resolution of current OCT systems.

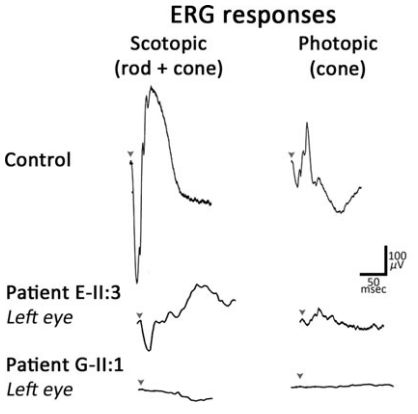

Fig. 5. ERG recordings of two patients with recordable responses. (patient E-II:3 at age 43 and G-II:1 at age 28). Only scotopic mixed (rod + cone) responses and photopic (cone) responses are depicted. Arrowheads indicate the moment of the light flash. Control shows normal responses of individuals with healthy retinas. Patient E-II:3 has severely reduced scotopic responses and photopic responses just within normal limits. Both dark-adapted and light-adapted responses of patient G-II:1 show barely detectable responses of <10 microvolts. ERG, electroretinography; ms, millisecond; μV, microvolts.

Genotype–phenotype analysis

All but one (B-II:9) patients demonstrated the slowly progressive, central-preserving retinal phenotype. Accordingly, the mutations identified in our patients (Table 3) all affect the kinase activity that is crucial for normal functioning of the MAK protein (Ozgul et al. 2011). Nonsense mutations, which are generally assumed to have more detrimental effects on protein

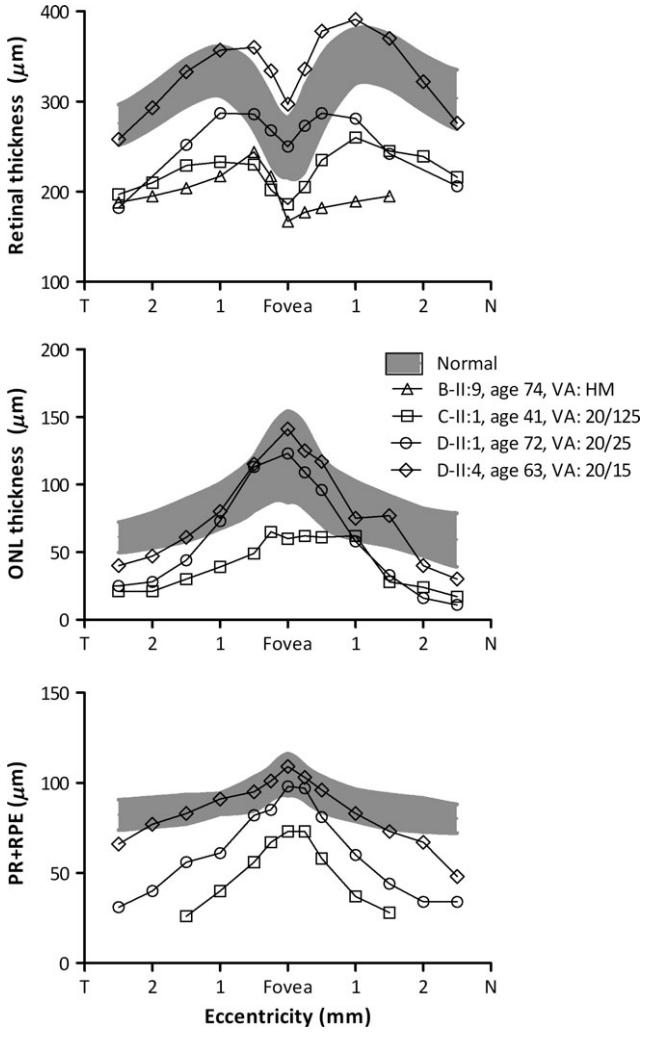

Fig. 7. Retinal laminar architecture by OCT in *MAK*-related RP. Thickness of the overall retina, ONL and photoreceptor–RPE complex (PR+RPE) along the horizontal meridian in four patients. In patient B-II:9, only the retinal thickness could be measured as unstable fixation led to low scan quality. Shaded areas: normal limits (mean ± 2 SD) as measured in 25 individuals without vitreoretinal and retinal disease (mean age: 46 year). VA, visual acuity; HM, hand movements.

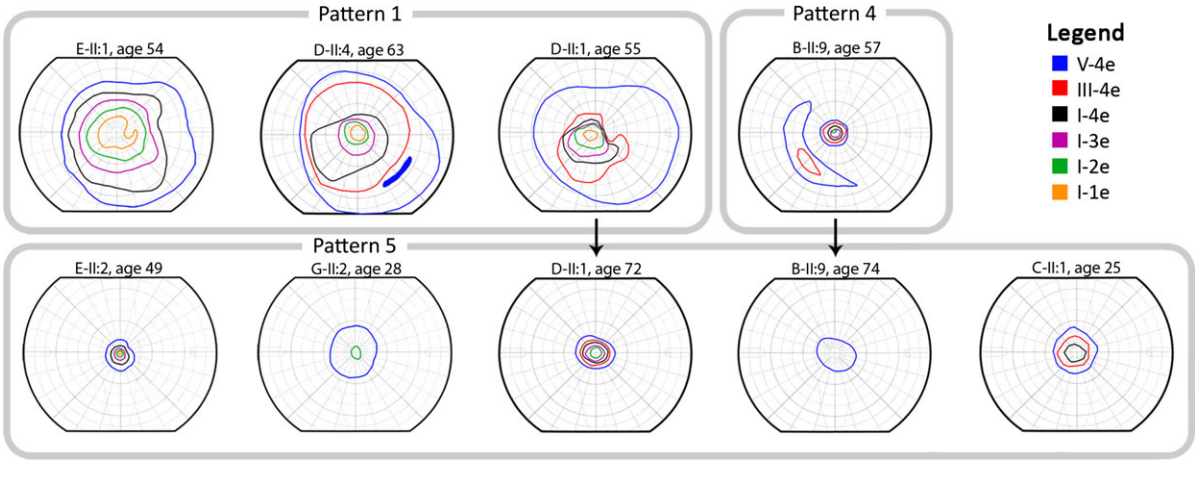

Fig. 6. Patterns of visual field loss by Goldmann kinetic perimetry. All fields are depicted as right eyes. Patterns are numbered according to Stone et al. (2011b). Pattern 1: Field show nearly full extent with the V-4e isopter and absolute scotoma, if present, are situated in the superotemporal quadrant. Pattern 4: isolation of the central field from the residual nasal field by a complete midperipheral scotoma. Pattern 5: only a residual small central island with V-4e and even smaller with I-4e. Fields are grouped by pattern. Patient ID and age are at the top of each map. Solid areas: absolute scotoma.

Table 2. UPSIT scores and interpretation of six patients with *MAK*-associated RP.

Patient	Age	UPSIT score	Percentile*	Absolute olfactory function corrected for age and gender
B-II:9	74	15/40	7th	Anosmia
C-II:3	41	32/40	13nd	Mild microsmia
D-II:1	72	26/40	17th	Moderate microsmia
D-II:4	63	36/40	53rd	Normosmia
E-II:1	54	33/40	17th	Mild microsmia
E-II:3	49	33/40	6th	Mild microsmia

* Percentiles indicate the percentage of normal individuals that reach an equal or lower score as the patient. UPSIT = University of Pennsylvania Smell Identification Test.

Table 3. Genetic findings in the patients included in this study.

	Allele 1		Allele 2			
Patient ID	Mutation	Effect	Mutation	Effect	Exon	Consanguinity
A-IV:1	c.718C → T	p.Gln240*	c.718C → T	p.Gln240*	8	First cousins
B-II:9	c.388A → C	p.Asn130His	c.388A → C	p.Asn130His	6	First cousins
C-II:3	c.37G → A	p.Gly13Ser	c.37G → A	p.Gly13Ser	2	First cousins
D-II:1	c.79G → A	p.Gly27Arg	NI	r.0	2	No
D-II:4	c.79G → A	p.Gly27Arg	NI	r.0	2	No
E-II:1	c.79G → C	p.Gly27Arg	c.542T → C	p.Ile181Thr	2, 7	No
E-II:3	c.79G → C	p.Gly27Arg	c.542T → C	p.Ile181Thr	2, 7	No
F-II:2	c.497G → A	p.Arg166His	c.497G → A	p.Arg166His	7	Yes
F-II:4	c.497G → A	p.Arg166His	c.497G → A	p.Arg166His	7	Yes
F-II:5	c.497G → A	p.Arg166His	c.497G → A	p.Arg166His	7	Yes
G-II:1	c.497G → A	p.Arg166His	c.497G → A	p.Arg166His	7	First cousins

NI = not identified.
*Premature protein termination.

function than missense changes, were identified in family A. However, the phenotype in patient A-IV:1 did not significantly differ from that in the other families. The p.Asn130His and p.Gly13Ser mutations, identified in B-II:9 and C-II:3, respectively, alter amino acids that are universally conserved across all known kinases (Hanks & Hunter 1995), and these mutant forms of MAK show virtually no kinase activity *in vitro* (Ozgul et al. 2011). However, the distinct retinal differences between these two patients suggest differences in the total mutational load elsewhere in the genome.

Variants in other retinal genes may have modified the phenotype in patient B-II:9. Prior to the identification of *MAK* mutations in patient B-II:9, targeted next generation sequencing in 111 known blindness genes had been performed (Neveling et al. 2012) (individual 9535 in this study). A heterozygous genetic variant was found in *GPR98*, which might have a modifying effect on the disease. Alternatively, modifier effects from variants in other (retinal) genes that were not analysed in the targeted next generation sequencing approach might be involved in the phenotype in patient B-II:9 as the atrophic macular phenotype deviates significantly from the relative preservation of macular function observed in the other patients. Additional genetic analysis with, for example, whole- exome sequencing may reveal pathologic mutations other than those present in *MAK*.

Although the absence of syndromic features is not uncommon in ciliary retinal disorders (Estrada-Cuzcano et al. 2012a,b,c), the question remains why syndromic features are absent while multiple tissues express *MAK*. Tissue-specific isoforms can result in disease features in only one tissue, and a retina-specific isoform of MAK, which includes an extra exon (exon 12 in that transcript) that is regulated by exon 9 (Tucker et al. 2011), has been described. However, none of the *MAK* mutations identified in our patients was located in either exon 9 or 12. Other explanations may include variance in levels of gene expression among tissues and the high metabolic rate of the retina compared with other tissues, potentially making the retina more prone to disruptive processes. Alternatively, we cannot completely rule out that we missed very subtle extra-ocular features.

MAK-related RP versus ciliopathies

To date, mutations in 34 ciliary genes have been associated with both syndromic and non-syndromic retinal disease (RetNet, available at https://sph.uth.edu/retnet/). Non-syndromic retinal disease is caused by defects in 24 of these genes, and the associated retinal phenotypes are summarized in Table S1 (except for the *MAK*-associated phenotype). Besides MAK, 13 ciliary genes are exclusively associated with non-syndromic retinal disease, without being associated with syndromic disease as well. Although detailed descriptions of most phenotypes associated with ciliary gene defects are lacking, we observed a remarkable clinical variability among non-syndromic ciliary retinal disease, ranging from relatively mild phenotypes like pericentral retinal dystrophy and occult macular dystrophy, to severe early-onset retinal degeneration phenotypes such as Leber congenital amaurosis (Table S1).

Non-syndromic RP forms caused by ciliary genes generally initiate during the first two decades of life and demonstrate reduced visual acuity as an early feature. Accordingly, profound macular atrophy is observed in a subset of these RP forms (Table S1). Mild RP phenotypes without early macular involvement are observed in retinal disease associated with mutations in *RP1*, *RP1L1*, *TOPORS* or *C2orf71* (Jacobson et al. 2000; Chakarova et al. 2007; Collin et al. 2010; Nishimura et al. 2010; Audo et al. 2012; Davidson et al. 2013b), which generally are adult-onset and characterized by a slow decline in visual acuity. As *RP1*, *RP1L1* and *TOPORS* are the only ciliary genes that cause non-syndromic dominant RP known to date, the classic dogma that dominantly inherited RP is milder compared with recessive and X-linked RP (Hartong et al. 2006) also applies when only ciliary RP is considered.

Like these dominantly inherited phenotypes, *MAK*-associated recessively

inherited RP resides at the mild end of the spectrum of diseases caused by ciliary genes. It shows remarkable resemblance to the phenotype observed in patients with *RP1* mutations in respect to the course of visual acuity loss, the patterns of retinal degeneration and visual field loss as described by Jacobson et al. (2000). Underlying mechanisms for the regional retinal variations have been optioned to lie in topographic characteristics in gene expression (Sakuta et al. 2001; Sharon et al. 2002; Cornish et al. 2005; Tanito et al. 2008), but further studies are necessary on this subject. The resemblance in phenotypes is especially intriguing as RP1 and MAK are functionally related: both proteins localize to the outer segment axoneme in murine photoreceptors, and RP1 is a phosphorylation target of MAK (Omori et al. 2010). Omori et al. suggested that phosphorylation of RP1 may influence microtubule stability and regulation of ciliary length. Moreover, if lack of RP1 phosphorylation is the direct cause of *MAK*-associated RP, this would also be in accordance with the absence of syndromic features, as *RP1* is expressed in the retina only (Sullivan et al. 1999).

In conclusion, we observed slowly progressive, autosomal recessive RP without syndromic features in patients with various nonsense or missense mutations in *MAK*. Visual acuity usually remains intact, although modifier effects may have negative consequences on central vision. *MAK*-associated RP is at the mild end of the ciliopathic RP phenotypes and shows remarkable resemblance to the retinal phenotype observed in *RP1*-related RP. Thus, defects in proteins that act in the pathway that involves MAK and RP1, may lead to relatively mild retinal phenotypes.

References

Abu Safieh L, Aldahmesh MA, Shamseldin H et al. (2010): Clinical and molecular characterisation of Bardet-Biedl syndrome in consanguineous populations: the power of homozygosity mapping. J Med Genet **47**: 236–241.

Abu-Safieh L, Al-Anazi S, Al-Abdi L et al. (2012): In search of triallelism in Bardet-Biedl syndrome. Eur J Hum Genet **20**: 420–427.

Ajmal M, Khan MI, Micheal S et al. (2012): Identification of recurrent and novel mutations in TULP1 in Pakistani families with early-onset retinitis pigmentosa. Mol Vis **18**: 1226–1237.

Akahori M, Tsunoda K, Miyake Y et al. (2010): Dominant mutations in RP1L1 are responsible for occult macular dystrophy. Am J Hum Genet **87**: 424–429.

Alazami AM, Alshammari MJ, Salih MA et al. (2012): Molecular characterization of Joubert syndrome in Saudi Arabia. Hum Mutat **33**: 1423–1428.

Aldahmesh MA, Safieh LA, Alkuraya H et al. (2009): Molecular characterization of retinitis pigmentosa in Saudi Arabia. Mol Vis **15**: 2464–2469.

Audo I, Mohand-Said S, Dhaenens CM et al. (2012): RP1 and autosomal dominant rod-cone dystrophy: novel mutations, a review of published variants, and genotype-phenotype correlation. Hum Mutat **33**: 73–80.

Bandah-Rozenfeld D, Mizrahi-Meissonnier L, Farhy C et al. (2010): Homozygosity mapping reveals null mutations in FAM161A as a cause of autosomal-recessive retinitis pigmentosa. Am J Hum Genet **87**: 382–391.

Bengs F, Scholz A, Kuhn D & Wiese M (2005): LmxMPK9, a mitogen-activated protein kinase homologue affects flagellar length in Leishmania mexicana. Mol Microbiol **55**: 1606–1615.

Berman SA, Wilson NF, Haas NA & Lefebvre PA (2003): A novel MAP kinase regulates flagellar length in Chlamydomonas. Curr Biol **13**: 1145–1149.

Bernal S, Ayuso C, Antinolo G et al. (2003): Mutations in USH2A in Spanish patients with autosomal recessive retinitis pigmentosa: high prevalence and phenotypic variation. J Med Genet **40**: e8.

Berson EL (1993): Retinitis pigmentosa. The Friedenwald Lecture. Invest Ophthalmol Vis Sci **34**: 1659–1676.

Blackshaw S, Harpavat S, Trimarchi J et al. (2004): Genomic analysis of mouse retinal development. PLoS Biol **2**: E247.

Bladt F & Birchmeier C (1993): Characterization and expression analysis of the murine rck gene: a protein kinase with a potential function in sensory cells. Differentiation **53**: 115–122.

Bowne SJ, Daiger SP, Malone KA et al. (2003): Characterization of RP1L1, a highly polymorphic paralog of the retinitis pigmentosa 1 (RP1) gene. Mol Vis **9**: 129–137.

Campo RV & Aaberg TM (1982): Ocular and systemic manifestations of the Bardet-Biedl syndrome. Am J Ophthalmol **94**: 750–756.

Cannon PS, Clayton-Smith J, Beales PL & Lloyd IC (2008): Bardet-biedl syndrome: an atypical phenotype in brothers with a proven BBS1 mutation. Ophthalmic Genet **29**: 128–132.

Chakarova CF, Papaioannou MG, Khanna H et al. (2007): Mutations in TOPORS cause autosomal dominant retinitis pigmentosa with perivascular retinal pigment epithelium atrophy. Am J Hum Genet **81**: 1098–1103.

Chen Y, Zhang Q, Shen T et al. (2013): Comprehensive mutation analysis by whole-exome sequencing in 41 Chinese families with Leber congenital amaurosis. Invest Ophthalmol Vis Sci **54**: 4351–4357.

Collin RW, Safieh C, Littink KW et al. (2010): Mutations in C2ORF71 cause autosomal-recessive retinitis pigmentosa. Am J Hum Genet **86**: 783–788.

Coppieters F, Casteels I, Meire F et al. (2010): Genetic screening of LCA in Belgium: predominance of CEP290 and identification of potential modifier alleles in AHI1 of CEP290-related phenotypes. Hum Mutat **31**: E1709–E1766.

Cornish EE, Madigan MC, Natoli R, Hales A, Hendrickson AE & Provis JM (2005): Gradients of cone differentiation and FGF expression during development of the foveal depression in macaque retina. Vis Neurosci **22**: 447–459.

Davidson AE, Schwarz N, Zelinger L et al. (2013a): Mutations in ARL2BP, encoding ADP-ribosylation-factor-like 2 binding protein, cause autosomal-recessive retinitis pigmentosa. Am J Hum Genet **93**: 321–329.

Davidson AE, Sergouniotis PI, Mackay DS et al. (2013b): RP1L1 variants are associated with a spectrum of inherited retinal diseases including retinitis pigmentosa and occult macular dystrophy. Hum Mutat **34**: 506–514.

De Lin W, Wang CH, Chou IC & Tsai FJ (2014): A novel one-base insertion mutation in the retinitis pigmentosa 2 gene in a large X-linked Taiwanese family. Acta Ophthalmol **92**: e161–e162.

Doty RL (1995): The Smell Identification Test Administration Manual (3rd edn.). Haddon Heights, NJ: Sensonics, Inc.

Estrada-Cuzcano A, Koenekoop RK, Coppieters F et al. (2011): IQCB1 mutations in patients with leber congenital amaurosis. Invest Ophthalmol Vis Sci **52**: 834–839.

Estrada-Cuzcano A, Koenekoop RK, Senechal A et al. (2012a): BBS1 mutations in a wide spectrum of phenotypes ranging from nonsyndromic retinitis pigmentosa to Bardet-Biedl syndrome. Arch Ophthalmol **130**: 1425–1432.

Estrada-Cuzcano A, Neveling K, Kohl S et al. (2012b): Mutations in C8orf37, encoding a ciliary protein, are associated with autosomal-recessive retinal dystrophies with early macular involvement. Am J Hum Genet **90**: 102–109.

Estrada-Cuzcano A, Roepman R, Cremers FP, den Hollander AI & Mans DA (2012c): Non-syndromic retinal ciliopathies: translating gene discovery into therapy. Hum Mol Genet **21**: R111–R124.

Eudy JD, Weston MD, Yao S et al. (1998): Mutation of a gene encoding a protein with extracellular matrix motifs in Usher syndrome type IIa. Science **280**: 1753–1757.

Fishman GA, Grover S, Jacobson SG, Alexander KR, Derlacki DJ, Wu W, Buraczynska M & Swaroop A (1998): X-linked retinitis pigmentosa in two families with a missense mutation in the RPGR gene and putative change of glycine to valine at codon 60. Ophthalmology **105**: 2286–2296.

Frank V, den Hollander AI, Bruchle NO et al. (2008): Mutations of the CEP290 gene encoding a centrosomal protein cause Meckel-Gruber syndrome. Hum Mutat **29**: 45–52.

Gerber S, Hanein S, Perrault I et al. (2007): Mutations in LCA5 are an uncommon cause of Leber congenital amaurosis (LCA) type II. Hum Mutat **28**: 1245.

Greenstein VC, Duncker T, Holopigian K, Carr RE, Greenberg JP, Tsang SH & Hood DC (2012): Structural and functional changes associated with normal and abnormal fundus autofluorescence in patients with retinitis pigmentosa. Retina **32**: 349–357.

Hameed A, Abid A, Aziz A, Ismail M, Mehdi SQ & Khaliq S (2003): Evidence of RPGRIP1 gene mutations associated with recessive cone-rod dystrophy. J Med Genet **40**: 616–619.

Hanks SK & Hunter T (1995): Protein kinases 6. The eukaryotic protein kinase superfamily: kinase (catalytic) domain structure and classification. FASEB J **9**: 576–596.

Hardcastle AJ, Thiselton DL, Zito I, Ebenezer N, Mah TS, Gorin MB & Bhattacharya SS (2000): Evidence for a new locus for X-linked retinitis pigmentosa (RP23). Invest Ophthalmol Vis Sci **41**: 2080–2086.

Hartong DT, Berson EL & Dryja TP (2006): Retinitis pigmentosa. Lancet **368**: 1795–1809.

Hildebrandt F, Benzing T & Katsanis N (2011): Ciliopathies. N Engl J Med **364**: 1533–1543.

Hoffman HJ, Cruickshanks KJ & Davis B (2009): Perspectives on population-based epidemiological studies of olfactory and taste impairment. Ann N Y Acad Sci **1170**: 514–530.

den Hollander AI, Koenekoop RK, Mohamed MD et al. (2007a): Mutations in LCA5, encoding the ciliary protein lebercilin, cause Leber congenital amaurosis. Nat Genet **39**: 889–895.

den Hollander AI, Lopez I, Yzer S et al. (2007b): Identification of novel mutations in patients with Leber congenital amaurosis and juvenile RP by genome-wide homozygosity mapping with SNP microarrays. Invest Ophthalmol Vis Sci **48**: 5690–5698.

den Hollander AI, van Lith-Verhoeven JJ, Arends ML, Strom TM, Cremers FP & Hoyng CB (2007c): Novel compound heterozygous TULP1 mutations in a family with severe early-onset retinitis pigmentosa. Arch Ophthal **125**: 932–935.

Huang WC, Wright AF, Roman AJ et al. (2012): RPGR-associated retinal degeneration in human X-linked RP and a murine model. Invest Ophthalmol Vis Sci **53**: 5594–5608.

van Huet RA, Estrada-Cuzcano A, Banin E et al. (2013): Clinical characteristics of rod and cone photoreceptor dystrophies in patients with mutations in the C8orf37 gene. Invest Ophthalmol Vis Sci **54**: 4683–4690.

Iannaccone A, Breuer DK, Wang XF et al. (2003): Clinical and immunohistochemical evidence for an X linked retinitis pigmentosa syndrome with recurrent infections and hearing loss in association with an RPGR mutation. J Med Genet **40**: e118.

Jacobson SG, Cideciyan AV, Iannaccone A et al. (2000): Disease expression of RP1 mutations causing autosomal dominant retinitis pigmentosa. Invest Ophthalmol Vis Sci **41**: 1898–1908.

Jayasundera T, Branham KE, Othman M, Rhoades WR, Karoukis AJ, Khanna H, Swaroop A & Heckenlively JR (2010): RP2 phenotype and pathogenetic correlations in X-linked retinitis pigmentosa. Arch Ophthalmol **128**: 915–923.

Khan MI, Kersten FF, Azam M et al. (2011): CLRN1 mutations cause nonsyndromic retinitis pigmentosa. Ophthalmology **118**: 1444–1448.

Khan AO, Abu-Safieh L, Eisenberger T, Bolz HJ & Alkuraya FS (2013): The RPGRIP1-related retinal phenotype in children. Br J Ophthalmol **97**: 760–764.

Langmann T, Di Gioia SA, Rau I et al. (2010): Nonsense mutations in FAM161A cause RP28-associated recessive retinitis pigmentosa. Am J Hum Genet **87**: 376–381.

Littink KW, Pott JW, Collin RW et al. (2010): A novel nonsense mutation in CEP290 induces exon skipping and leads to a relatively mild retinal phenotype. Invest Ophthalmol Vis Sci **51**: 3646–3652.

Marmor MF, Fulton AB, Holder GE, Miyake Y, Brigell M & Bach M (2009): ISCEV Standard for full-field clinical electroretinography (2008 update). Doc Ophthalmol **118**: 69–77.

Matsushime H, Jinno A, Takagi N & Shibuya M (1990): A novel mammalian protein kinase gene (mak) is highly expressed in testicular germ cells at and after meiosis. Mol Cell Biol **10**: 2261–2268.

McEwen DP, Koenekoop RK, Khanna H, Jenkins PM, Lopez I, Swaroop A & Martens JR (2007): Hypomorphic CEP290/NPHP6 mutations result in anosmia caused by the selective loss of G proteins in cilia of olfactory sensory neurons. Proc Natl Acad Sci U S A **104**: 15917–15922.

McKibbin M, Ali M, Mohamed MD et al. (2010): Genotype-phenotype correlation for leber congenital amaurosis in Northern Pakistan. Arch Ophthal **128**: 107–113.

Mockel A, Perdomo Y, Stutzmann F, Letsch J, Marion V & Dollfus H (2011): Retinal dystrophy in Bardet-Biedl syndrome and related syndromic ciliopathies. Prog Retin Eye Res **30**: 258–274.

Moore A, Escudier E, Roger G et al. (2006): RPGR is mutated in patients with a complex X linked phenotype combining primary ciliary dyskinesia and retinitis pigmentosa. J Med Genet **43**: 326–333.

Neveling K, Collin RW, Gilissen C et al. (2012): Next generation genetic testing for retinitis pigmentosa. Hum Mutat **33**: 963–972.

Nigg EA & Raff JW (2009): Centrioles, centrosomes, and cilia in health and disease. Cell **139**: 663–678.

Nishiguchi KM, Tearle RG, Liu YP et al. (2013): Whole genome sequencing in patients with retinitis pigmentosa reveals pathogenic DNA structural changes and NEK2 as a new disease gene. Proc Natl Acad Sci U S A **110**: 16139–16144.

Nishimura DY, Baye LM, Perveen R et al. (2010): Discovery and functional analysis of a retinitis pigmentosa gene, C2ORF71. Am J Hum Genet **86**: 686–695.

Novarino G, Akizu N & Gleeson JG (2011): Modeling human disease in humans: the ciliopathies. Cell **147**: 70–79.

Omori Y, Chaya T, Katoh K et al. (2010): Negative regulation of ciliary length by ciliary male germ cell-associated kinase (Mak) is required for retinal photoreceptor survival. Proc Natl Acad Sci U S A **107**: 22671–22676.

Ozgul RK, Siemiatkowska AM, Yucel D et al. (2011): Exome sequencing and cis-regulatory mapping identify mutations in MAK, a gene encoding a regulator of ciliary length, as a cause of retinitis pigmentosa. Am J Hum Genet **89**: 253–264.

Perrault I, Delphin N, Hanein S et al. (2007): Spectrum of NPHP6/CEP290 mutations in Leber congenital amaurosis and delineation of the associated phenotype. Hum Mutat **28**: 416.

Ponjavic V, Andreasson S, Abrahamson M, Ehinger B, Gieser L, Fujita R & Swaroop A (1998): Clinical expression of X-linked retinitis pigmentosa in a Swedish family with the RP2 genotype. Ophthalmic Genet **19**: 187–196.

Popovic P, Jarc-Vidmar M & Hawlina M (2005): Abnormal fundus autofluorescence in relation to retinal function in patients with retinitis pigmentosa. Graefes Arch Clin Exp Ophthalmol **243**: 1018–1027.

Riazuddin SA, Iqbal M, Wang Y et al. (2010): A splice-site mutation in a retina-specific exon of BBS8 causes nonsyndromic retinitis pigmentosa. Am J Hum Genet **86**: 805–812.

Roosing S, Rohrschneider K, Beryozkin A et al. (2013a): Mutations in RAB28, encoding a farnesylated small GTPase, are associated with autosomal-recessive cone-rod dystrophy. Am J Hum Genet **93**: 110–117.

Roosing S, van den Born LI, Hoyng CB et al. (2013b): Maternal uniparental isodisomy of chromosome 6 reveals a TULP1 mutation as a novel cause of cone dysfunction. Ophthalmology **120**: 1239–1246.

Rosenberg T, Schwahn U, Feil S & Berger W (1999): Genotype-phenotype correlation in X-linked retinitis pigmentosa 2 (RP2). Ophthalmic Genet **20**: 161–172.

Sakuta H, Suzuki R, Takahashi H et al. (2001): Ventroptin: a BMP-4 antagonist expressed in a double-gradient pattern in the retina. Science **293**: 111–115.

Sandberg MA, Rosner B, Weigel-DiFranco C, Dryja TP & Berson EL (2007): Disease course of patients with X-linked retinitis pigmentosa due to RPGR gene mutations. Invest Ophthalmol Vis Sci **48**: 1298–1304.

Schwartz SB, Aleman TS, Cideciyan AV et al. (2005): Disease expression in Usher syndrome caused by VLGR1 gene mutation (USH2C) and comparison with USH2A phenotype. Invest Ophthalmol Vis Sci **46**: 734–743.

Selmer KK, Grondahl J, Riise R, Brandal K, Braaten O, Bragadottir R & Undlien DE (2010): Autosomal dominant pericentral retinal dystrophy caused by a novel missense mutation in the TOPORS gene. Acta Ophthalmol **88**: 323–328.

Sharon D, Blackshaw S, Cepko CL & Dryja TP (2002): Profile of the genes expressed in the human peripheral retina, macula, and retinal pigment epithelium determined through serial analysis of gene expression (SAGE). Proc Natl Acad Sci U S A **99**: 315–320.

Shinkai Y, Satoh H, Takeda N, Fukuda M, Chiba E, Kato T, Kuramochi T & Araki Y (2002): A testicular germ cell-associated serine-threonine kinase, MAK, is dispensable for sperm formation. Mol Cell Biol **22**: 3276–3280.

Stone EM, Cideciyan AV, Aleman TS et al. (2011a): Variations in NPHP5 in patients with nonsyndromic leber congenital amaurosis and Senior-Loken syndrome. Arch Ophthal **129**: 81–87.

Stone EM, Luo X, Heon E et al. (2011b): Autosomal recessive retinitis pigmentosa caused by mutations in the MAK gene. Invest Ophthalmol Vis Sci **52**: 9665–9673.

Sullivan LS, Heckenlively JR, Bowne SJ et al. (1999): Mutations in a novel retina-specific gene cause autosomal dominant retinitis pigmentosa. Nat Genet **22**: 255–259.

Tanito M, Kaidzu S, Ohira A & Anderson RE (2008): Topography of retinal damage in light-exposed albino rats. Exp Eye Res **87**: 292–295.

Thiadens AA, Soerjoesing GG, Florijn RJ et al. (2011): Clinical course of cone dystrophy caused by mutations in the RPGR gene. Graefes Arch Clin Exp Ophthalmol **249**: 1527–1535.

Tucker BA, Scheetz TE, Mullins RF et al. (2011): Exome sequencing and analysis of induced pluripotent stem cells identify the cilia-related gene male germ cell-associated kinase (MAK) as a cause of retinitis pigmentosa. Proc Natl Acad Sci U S A **108**: E569–E576.

Walia S, Fishman GA, Jacobson SG et al. (2010): Visual acuity in patients with Leber's congenital amaurosis and early childhood-onset retinitis pigmentosa. Ophthalmology **117**: 1190–1198.

Webb TR, Parfitt DA, Gardner JC et al. (2012): Deep intronic mutation in OFD1, identified by targeted genomic next-generation sequencing, causes a severe form of X-linked retinitis pigmentosa (RP23). Hum Mol Genet **21**: 3647–3654.

Yzer S, Hollander AI, Lopez I, Pott JW, de Faber JT, Cremers FP, Koenekoop RK & van den Born LI (2012): Ocular and extra-ocular features of patients with Leber congenital amaurosis and mutations in CEP290. Mol Vis **18**: 412–425.

Zito I, Downes SM, Patel RJ et al. (2003): RPGR mutation associated with retinitis pigmentosa, impaired hearing, and sinorespiratory infections. J Med Genet **40**: 609–615.

Received on January 8th, 2014.
Accepted on June 17th, 2014.

Correspondence
B. J. Klevering
Department of Ophthalmology
Radboud University Medical Center
Philips van Leydenlaan 15
Nijmegen 6525 EX
The Netherlands
Tel: +31(0) 24 361 44 48
Fax: +31 (0) 24 354 05 22
Email: Jeroen.Klevering@radboudumc.nl

We gratefully acknowledge all patients included in this study. We also thank Patricia Stappers for her help regarding administration of the smell test, Michel Teussink for assistance with MatLab and Eefje Buijnster for the additional genetic tests. This study was supported by the Stichting A.F. Deutman Researchfonds Oogheelkunde, Nijmegen, The Netherlands, the Foundation Fighting Blindness USA (FFB Grant numbers C-GE-0811-0545-RAD01 and BR-GE-0510-0489-RAD) and The Netherlands Organization for Health Research and Development (ZonMW; TOP-grant 40-00812-98-09047). The funding organizations had no role in the design or conduct of this research. No conflicting relationship exists for any author.

Supporting Information

Additional Supporting Information may be found in the online version of this article:

Table S1. General phenotypic features of non-syndromic ciliopathic retinal dystrophies.